

BINUCLEAR-TRANSITION METAL COMPLEXES CONTAINING 6 N MOIETIES SCHIFF BASE LIGAND: SYNTHESIS, CHARACTERIZATION AND MICROBICIDE ACTIVITIES

Sabreen Mohamed Elgamasy^{1*} and Samar Ebrahim Abd-ElRazek²

¹Department of Chemistry, Faculty of Science, El-Menoufia University, Shebin El-Kom, Egypt

²Clinical Pathology Department, National Liver Institute, Menoufia University, Shebin El-Kom

(Received November 21, 2022; Revised February 20, 2023; Accepted February 21, 2023)

ABSTRACT. Complexes of Co(II), Ni(II) and Cu(II) ions with tetra amine hydrazide ligand [H₄L] were prepared and characterized using physical and spectral methods. Analytical data showed that the complexes found in (1:2) ligand:metal ratio. Spectral studies revealed that the ligand bonded to the metal ion in neutral tetradentate or tetrabasic tetradentate manner through azomethine nitrogen atom, protonated/deprotonated hydroxyl group. From the electronic spectral data together with magnetic susceptibility values a distorted octahedral structure can be proposed for all complexes except complex **2** which has square planar structure. Electron spin resonance spectra for Co(II) complex **6** revealed axial symmetry with $g_{\parallel} > g_{\perp} > g_e$, indicating distorted octahedral or square planar structures and the unpaired electron exists in a $d(x^2-y^2)$ orbital with marked covalent bond feature. Quantum chemical calculations have been performed to study structures and energetics of the ligand and its complexes. The prepared complexes showed good to excellent antimicrobial activity, and the most active complexes against *Aspergillus niger* were **3** with zone of inhibition of 23 mm. Complex **7** showed interesting activity against *Escherichia coli* with zone of inhibition of 23 mm.

KEY WORDS: Metal complexes, Nitrogen moiety, Antimicrobicide activity

INTRODUCTION

Schiff bases derived from an amino and carbonyl compound are an important class of ligands that coordinate to metal ions via azomethine nitrogen and have been studied extensively. In azomethine derivatives, the C=N linkage is essential for biological activity, several azomethine have been reported to possess remarkable antibacterial, antifungal, anticancer and antimalarial activities [1], which leads to great in vivo stability and generally, a lack of toxicity for higher vertebrates, including humans. The incorporated metals in the lattice of donor atoms of Schiff base change the physiological, morphological, and pharmacological activities of the compounds. The Schiff base compounds are of promising research interest owing to the widespread antibacterial resistance of the medical science. Moreover, the revival of research is essential to generate new Schiff base metal complexes with a diverse range of applications. Schiff base complexes have been used as drugs and have valuable antibacterial [2, 3], antifungal [4-6], antiviral [7, 8], anti-inflammatory [9], and antitumor activities [10]. Besides these, they also bear strong catalytic activity in various chemical reactions in chemistry [11]. It is a broad spectrum, semisynthetic penicillin type antibiotic that has potent bactericidal activity against many gram positive and gram negative bacterial pathogens [12]. It takes action against bacteria by preventing them from forming the cell wall and stopping them from growing. In medical science, it has important application for the treatment of bronchitis, ear infection, pneumonia, throat infections, tonsillitis, typhoid, and urinary tract infections. In combination with other antibiotics, it bears potential applications for the successful treatment of many pathogenic infections.

*Corresponding author. E-mail: sabreen_mohamed2008@yahoo.com

This work is licensed under the Creative Commons Attribution 4.0 International License

In this study, a new Schiff base ligand was synthesized by condensation of 2,2'-(1,4-phenylene)diguandine and 2-hydroxybenzaldehyde (salicylaldehyde). The new ligand was reacted with Co(II), Ni(II) and Cu(II) ions to afford the corresponding metal complexes. Moreover, the preliminary in vitro antibacterial screening activities of the complexes obtained are carried out and the results are reported herein.

EXPERIMENTAL

Analytical and physical measurements

All the reagents were of the best grade available and used without further purification. C, H and N analyses were determined at the Analytical Unit of Cairo University, Egypt. A standard gravimetric method was used to determine metal ion [13]. All metal complexes were dried under vacuum over P₄O₁₀. The IR spectra were measured as KBr pellets using a Perkin-Elmer 683 spectrophotometer (4000-200 cm⁻¹). Electronic spectra (qualitatively) were recorded on a Perkin-Elmer 550 spectrophotometer. The conductance of 10⁻³ M solutions of the complexes in DMF were measured at 25 °C with a Bibby conductimeter type MCI. ¹H-NMR spectra (ligand and its Cu(II) and Zn(II) complexes) were obtained with Perkin-Elmer R32-90-MHz spectrophotometer using TMS as internal standard. Mass spectrum of the ligand was recorded using JEULJMS-AX-500 mass spectrometer provided with data system. The thermal analyses (DTA and TGA) were carried out in air on a Shimadzu DT-30 thermal analyzer from 27 to 800 °C at a heating rate of 10 °C per min. Magnetic susceptibilities were measured at 25 °C by the Gouy method using mercuric tetrathiocyanato cobalt(II) as the magnetic susceptibility standard. Diamagnetic corrections were estimated from Pascal's constant [14]. The magnetic moments were calculated

from the equation: $\mu_{eff} = 2.84 \sqrt{\chi_M^{corr} \cdot T}$. The ESR spectra of solid complexes at room temperature were recorded using a Varian E-109 spectrophotometer, DPPH was used as a standard material. The TLC of all compounds confirmed their purity.

Synthesis of Ligand (H₄L) (I)

1,4-Phenylenediamine (5.00 g, 0.0463 mol) and thiourea (7.04 g, .0923 mol) by (1:2) molar ratio, were dissolved in 50 mL of EtOH then two drops of glacial acetic acid was added and the mixture was refluxed until the reaction was completed. After cooling to room temperature, the solid was filtered. The precipitate was washed with ethanol to afford the corresponding hydrazide (2,2'-(1,4-phenylene)diguandine). The second step containing the addition of salicylaldehyde (25.6 g, 0.2128 mol) to the (2,2'-(1,4-phenylene)diguandine) (10 g, 0.0532 mol) by (4:1) molar ratio and the mixture was refluxed for 4- 6 hours until the final product is obtained as a grey solid material. The resulting solid was filtered and washed several times with ethanol and then dried under vacuum (Scheme 1). With m.p. 250 °C. Elemental analysis for C₃₆H₂₄N₆O₄ (85) (%): found (calcd): C, 71.99 (71.52); H, 3.83 (3.97); N, 13.99 (19.92). IR (KBr, cm⁻¹), 3440/3550–3150 ν(OH/H₂O), 1360 ν(C–O), 1635, 1615 ν(C=N)azo, 1570, 755 ν(Ar)_{ring}, ¹H NMR (600 MHz, DMSO-*d*₆, δ, ppm): 5.0 (s, 4 H, OH_{salicylaldehyde}), 8.20–6.80 (m, 20 H, C-H, aromatic).

Synthesis of H₄L ligand metal complexes

The complexes (2–7) were prepared by adding metal salts [Cu(CH₃COO)₂·2H₂O, CuCl₂, [Ni(CH₃COO)₂·6H₂O, NiCl₂·6H₂O, [Co(CH₃COO)₂·6H₂O and CoCl₂·6H₂O (2 mol, in 50 mL of ethanol) to ligand [H₄L] (2 g, 1 mol, in 50 mL of absolute ethanol) in the presence or absence of 2 mL of triethylamine. The mixture was refluxed for 5 h with stirring. The resulting solid complexes were filtered off while heated, washed several times with hot ethanol and finally dried over P₄O₁₀.

Cu⁺² complex (2). Yield (65%); m.p. > 300 °C; colour: dark green; $\mu_{\text{eff}} = 1.72$; molar conductivity (Λ_m): $16.1 \Omega^{-1} \text{ cm}^2 \text{ mol}^{-1}$. Elemental analysis for $[(\text{L})\text{Cu}_2(\text{H}_2\text{O})_4]\cdot\text{H}_2\text{O}$, $\text{C}_{36}\text{H}_{34}\text{Cu}_2\text{N}_6\text{O}_9$ (822): found (calcd): C, 52.62 (52.82); H, 4.17 (3.97); N, 10.23 (10.05); Cu, 15.47 (15.35). IR (KBr, cm^{-1}), 3380/3600–3320 $\nu(\text{OH}/\text{H}_2\text{O})$, 1340 $\nu(\text{C}-\text{O})$, 1620, 1605 $\nu(\text{C}=\text{N})_{\text{azo}}$, 1590, 750 $\nu(\text{Ar})_{\text{ring}}$, 580 $\nu(\text{Cu}-\text{O})$, 427 $\nu(\text{Cu}-\text{N})$.

Cu⁺² complex (3). Yield (65%); m.p. > 300 °C; colour: dark green; $\mu_{\text{eff}} = 1.73$; molar conductivity (Λ_m): $10.4 \Omega^{-1} \text{ cm}^2 \text{ mol}^{-1}$. Elemental analysis for $[(\text{L})\text{Cu}_2(\text{H}_2\text{O})_4]\cdot\text{H}_2\text{O}$, $\text{C}_{36}\text{H}_{32}\text{Cl}_4\text{Cu}_2\text{N}_6\text{O}_6$ (914): found (calcd): C, 47.33 (47.52); H, 3.53 (3.38); N, 9.20 (9.24); Cu, 13.91 (13.88); Cl, 15.52 (15.62). IR (KBr, cm^{-1}), 3370/3515–3220 $\nu(\text{OH}/\text{H}_2\text{O})$, 1322 $\nu(\text{C}-\text{O})$, 1625, 1610 $\nu(\text{C}=\text{N})_{\text{azo}}$, 1570, 745 $\nu(\text{Ar})_{\text{ring}}$, 560 $\nu(\text{Cu}-\text{O})$, 427 $\nu(\text{Cu}-\text{N})$ and 420 $\nu(\text{Cu}-\text{Cl})$.

Ni²⁺ complex (4). Yield (73%); m.p. > 300 °C; colour: brown; $\mu_{\text{eff}} = \text{dia.}$; molar conductivity (Λ_m): $13.2 \Omega^{-1} \text{ cm}^2 \text{ mol}^{-1}$. Elemental analysis for $[(\text{H}_4\text{L})\text{Ni}_2(\text{OAc})_4]\cdot\text{H}_2\text{O}$, $\text{C}_{44}\text{H}_{42}\text{Ni}_2\text{N}_6\text{O}_{13}$ (980): found (calcd): C, 53.91 (54.14); H, 4.32 (4.15); N, 8.57 (8.61); Ni, 11.98 (12.02). IR (KBr, cm^{-1}), 3390/3560–3225 $\nu(\text{OH}/\text{H}_2\text{O})$, 1325 $\nu(\text{C}-\text{O})$, 1615, 1600 $\nu(\text{C}=\text{N})_{\text{imine}}$, 1560, 764 745 $\nu(\text{Ar})_{\text{ring}}$, 1550/1349 $\nu(\text{CH}_3\text{COO})$, 519 $\nu(\text{Ni}-\text{O})$, 455 $\nu(\text{Ni}-\text{N})$.

Ni²⁺ complex (5). Yield (71%); m.p. > 300 °C; colour: brown; $\mu_{\text{eff}} = \text{dia.}$; molar conductivity (Λ_m): $14.3 \Omega^{-1} \text{ cm}^2 \text{ mol}^{-1}$. Elemental analysis for $[(\text{H}_4\text{L})\text{Ni}_2(\text{Cl})_4]\cdot 3\text{H}_2\text{O}$, $\text{C}_{36}\text{H}_{34}\text{Cl}_4\text{Ni}_2\text{N}_6\text{O}_7$ (921): found (calcd): C, 46.90 (47.1); H, 3.72 (3.57); N, 9.12 (9.16); Ni, 12.73 (12.78); Cl, 15.38 (15.45). IR (KBr, cm^{-1}), 3370/3640–3265 $\nu(\text{OH}/\text{H}_2\text{O})$, 1345 $\nu(\text{C}-\text{O})$, 1620, 1605 $\nu(\text{C}=\text{N})_{\text{imine}}$, 1573, 753 $\nu(\text{Ar})_{\text{ring}}$, 555 $\nu(\text{Ni}-\text{O})$, 468 $\nu(\text{Ni}-\text{N})$, 418 $\nu(\text{Ni}-\text{Cl})$.

Co²⁺ complex (6). Yield (66%); m.p. > 300 °C; colour: dark red; $\mu_{\text{eff}} = 3.99$; molar conductivity (Λ_m): $6.5 \Omega^{-1} \text{ cm}^2 \text{ mol}^{-1}$. Elemental analysis for $[(\text{H}_4\text{L})\text{Co}_2(\text{OAc})_4]\cdot\text{H}_2\text{O}$, $\text{C}_{44}\text{H}_{42}\text{N}_6\text{Co}_2\text{O}_{13}$ (981): found (calcd): C, 53.89 (54.11); H, 4.32 (3.89); N, 8.57 (8.61); Co, 12.02 (12.1). IR (KBr, cm^{-1}), 3410/3620–3210 $\nu(\text{OH}/\text{H}_2\text{O})$, 1335 $\nu(\text{C}-\text{O})$, 1626, 1608 $\nu(\text{C}=\text{N})_{\text{imine}}$, 1573, 760 $\nu(\text{Ar})_{\text{ring}}$, 545 $\nu(\text{Co}-\text{O})$, 458 $\nu(\text{Co}-\text{N})$.

Co²⁺ complex (7). Yield (63%); m.p. > 300 °C; colour: dark red; $\mu_{\text{eff}} = 3.85$; molar conductivity (Λ_m): $11.6 \Omega^{-1} \text{ cm}^2 \text{ mol}^{-1}$. Elemental analysis for $[(\text{H}_4\text{L})\text{Co}_2(\text{Cl})_4]\cdot 2\text{H}_2\text{O}$, $\text{C}_{36}\text{H}_{32}\text{Cl}_4\text{Co}_2\text{N}_6\text{O}_6$ (904): found (calcd): C, 47.81 (48.5); H, 3.57 (3.17); N, 9.29 (9.34); Co, 13.03 (13.09); Cl, 15.68 (15.57). IR (KBr, cm^{-1}), 3420/3620–3255 $\nu(\text{OH}/\text{H}_2\text{O})$, 1342 $\nu(\text{C}-\text{O})$, 1618, 1609 $\nu(\text{C}=\text{N})_{\text{imine}}$, 1565, 770 $\nu(\text{Ar})_{\text{ring}}$, 550 $\nu(\text{Co}-\text{O})$, 450 $\nu(\text{Co}-\text{N})$, 415 $\nu(\text{Co}-\text{Cl})$.

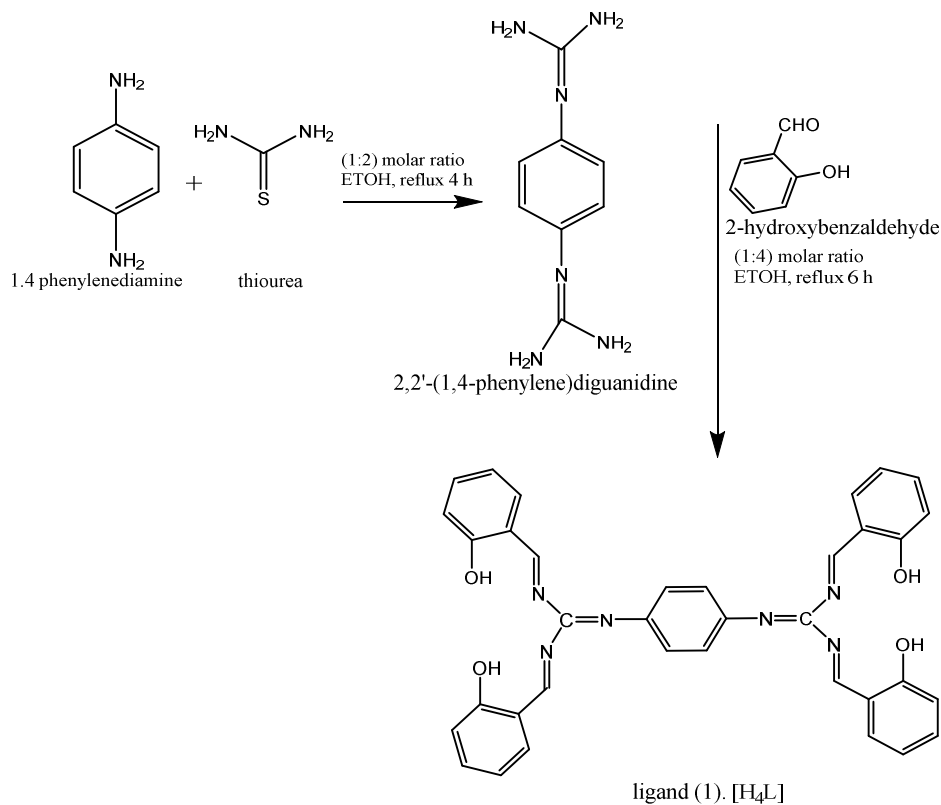
Biological activity

The well diffusion method was used to measure the antimicrobial activity [15-18]. Both positive (amphotericin B for fungi, tetracycline for bacteria) and negative (solvent, DMSO) controls were used in the technique. The complexes and ligand were tested against *Aspergillus niger* fungi and *Escherichia coli* bacteria cultured on Czapek Dox agar and nutrient agar as media, respectively. In a typical procedure, a well was made in the agar medium inoculated with the fungi or bacteria. The well was filled with the test solution (20 mg ml^{-1}) using a micropipette and the plate were incubated at 37 °C for 72 h. During the test the solution diffused and the growth of the inoculated fungi or bacteria was affected. The inhibition zone developed on the plate was recorded. Each test was conducted three times and the activity index for the complexes was calculated using the following formula:

Activity index = (Diameter of inhibition zone for test compound/Diameter of inhibition zone for standard) \times 100

RESULTS AND DISCUSSION*Chemistry*

The preparation of the new ligand (H_4L) involved two steps as illustrated in Scheme 1. Initially 1,4-phenylenediamine reacts with thiourea in (1:2) molar ratio affords 2,2'-(1,4-phenylene)diguandine, which then reacts with salicylaldehyde at molar ratio (1:4) to give the novel Schiff base ligand (H_4L). The structure of the ligand was elucidated using elemental analysis and spectral methods. Moreover, the ligand was utilized for chelation with various metal(II) salts. The analytical and physical data (Table 1), spectral data (Tables 2 and 3) showed that, the complexes are formed in (1L:2M) stoichiometric ratio. All the complexes are stable at room temperature, insoluble in common solvents, viz: MeOH, EtOH, $CHCl_3$, CCl_4 and $(CH_3)_2CO$ but soluble in DMSO [12, 13]. Ligand [H_4L] (**1**), was synthesized by condensation of tetraamine hydrazide with salicylaldehyde (1:4) molar ratio as shown in Figure 1.



Scheme 1. Preparation of ligand (H_4L).

Table 1. Analytical and physical data of the ligand [H₄L] and its metal complexes.

No.	Ligand/Complexes	Color	FW	m.p. (°C)	Yield (%)	Anal./Found (Calc.) (%)					Molar conductance Λ_m ($\Omega^{-1} \text{cm}^2 \text{mol}^{-1}$)
						C	H	N	M	Cl	
(1)	[H ₄ L] C ₃₆ H ₂₄ N ₆ O ₄	Grey	604	250	85	71.99 (71.52)	3.83 (3.97)	13.99 (13.91)	-	-	-
(2)	[(L)Cu ₂].4H ₂ O C ₃₆ H ₃₀ Cu ₂ N ₆ O ₇	Dark green	802	>300	65	54.95 (53.80)	4.02 (4.01)	10.58 (10.46)	16.07 (15.81)	-	16.1
(3)	[(H ₄ L)Cu ₂ (Cl) ₄].2H ₂ O C ₃₆ H ₃₂ Cl ₄ Cu ₂ N ₆ O ₆	Dark green	914	>300	65	47.33 (47.52)	3.53 (3.38)	9.20 (9.24)	13.91 (13.88)	15.52 (15.62)	10.4
(4)	[(H ₄ L)Ni ₂ (OAc) ₄].H ₂ O C ₄₄ H ₄₂ Ni ₂ N ₆ O ₁₃	Brown	980	>300	73	53.91 (54.14)	4.32 (4.15)	8.57 (8.61)	11.98 (12.02)	-	13.2
(5)	[(H ₄ L)Ni ₂ (Cl) ₄].3H ₂ O C ₃₆ H ₃₄ Cl ₄ Ni ₂ N ₆ O ₇	Brown	921	>300	71	46.90 (47.1)	3.72 (3.57)	9.12 (9.16)	12.73 (12.78)	15.38 (15.45)	14.3
(6)	[(H ₄ L)Co ₂ (OAc) ₄].H ₂ O C ₄₄ H ₄₂ N ₆ Co ₂ O ₁₃	Dark red	981	>300	66	53.89 (54.11)	4.32 (3.89)	8.57 (8.61)	12.02 (12.1)	-	16.5
(7)	[(H ₄ L)Co ₂ (Cl) ₄].2H ₂ O C ₃₆ H ₃₂ Cl ₄ Co ₂ N ₆ O ₆	Dark red	904	>300	63	47.81 (48.5)	3.57 (3.17)	9.29 (9.34)	13.03 (13.09)	15.68 (15.73)	11.6

Table 2. Mass spectra of ligand(1) and its complexes.

Complex No.	Fragment	m/z	Rel. Int.
(1)	C ₆ H ₅ O	93	13
	C ₇ H ₅ ON	119	16
	C ₈ H ₅ ON	131	20
	C ₉ H ₅ N ₂ O	157	22
	C ₁₅ H ₁₀ N ₂ O ₂	250	14
	C ₁₅ H ₁₀ N ₃ O ₂	264	25
	C ₂₁ H ₁₄ N ₃ O ₂	340	10
	C ₂₂ H ₁₄ N ₄ O ₂	366	11
	C ₂₃ H ₁₄ N ₅ O ₂	392	27
	C ₂₉ H ₁₉ N ₅ O ₃	485	29
	C ₃₀ H ₁₉ N ₆ O ₃	511	16
(2)	C ₃₆ H ₂₄ N ₆ O ₄	604	14
	C ₇ H ₆ NO ₂	136	21
	C ₁₁ H ₁₂ NO ₆ Cu	317.5	13
	C ₁₈ H ₁₆ N ₂ O ₇ Cu	435.5	25
	C ₁₉ H ₁₆ N ₃ O ₇ Cu	461.5	27
	C ₂₅ H ₂₀ N ₃ O ₇ Cu	537.5	24
	C ₂₆ H ₂₀ N ₄ O ₈ Cu	563.5	22
	C ₃₃ H ₂₄ N ₅ O ₈ Cu	681.5	23
(3)	C ₃₄ H ₃₀ N ₅ O ₁₂ Cu ₂	827	15
	C ₃₆ H ₃₀ Cu ₂ N ₆ O ₇	785.7	16
	C ₇ H ₉ NO ₃	155	15
	C ₇ H ₉ NO ₃ Cl ₂ Cu	289.5	17
	C ₁₄ H ₄ N ₂ O ₄ Cl ₂ Cu	408.5	18
	C ₁₅ H ₁₄ N ₃ O ₄ Cl ₂ Cu	434.5	20
	C ₂₁ H ₁₈ N ₃ O ₄ Cl ₂ Cu	510.5	21
	C ₂₂ H ₁₈ N ₄ O ₄ Cl ₂ Cu	536.5	23
	C ₂₉ H ₂₃ N ₅ O ₅ Cl ₂ Cu	655.5	16
	C ₂₉ H ₂₃ N ₅ O ₅ Cl ₄ Cu ₂	790	19
(4)	C ₃₀ H ₂₃ N ₆ O ₅ Cl ₄ Cu ₂	816	25
	C ₃₆ H ₂₈ N ₆ O ₆ Cl ₄ Cu ₂	909	27
	C ₇ H ₇ NO ₂	137	17

	C ₁₁ H ₁₃ NO ₆ Ni	301.6	18
	C ₁₈ H ₁₈ N ₂ O ₇ Ni	432.6	22
	C ₁₉ H ₁₈ N ₃ O ₇ Ni	458.6	24
	C ₂₅ H ₂₂ N ₃ O ₇ Ni	534.6	21
	C ₂₆ H ₂₂ N ₄ O ₇ Ni	560.6	20
	C ₃₃ H ₂₇ N ₅ O ₈ Ni	679.6	19
	C ₃₇ H ₃₃ N ₅ O ₁₂ Ni ₂	855	18
	C ₄₄ H ₃₈ N ₆ O ₁₃ Ni ₂	975.2	17
(5)	C ₇ H ₁₁ NO ₄	173	16
	C ₇ H ₁₁ NO ₄ Cl ₂ Ni	302.6	18
	C ₁₄ H ₁₆ N ₂ O ₅ Cl ₂ Ni	421.6	10
	C ₁₅ H ₁₆ N ₃ O ₅ Cl ₂ Ni	447.6	14
	C ₂₁ H ₂₀ N ₃ O ₅ Cl ₂ Ni	523.6	16
	C ₂₂ H ₂₀ N ₄ O ₅ Cl ₂ Ni	549.6	17
	C ₂₉ H ₂₅ N ₅ O ₆ Cl ₂ Ni	668.6	22
	C ₂₉ H ₂₅ N ₅ O ₆ Cl ₄ Ni ₂	798.2	28
	C ₃₆ H ₃₀ N ₆ O ₇ Cl ₄ Ni ₂	917.2	24
(6)	C ₇ H ₇ NO ₂	137	17
	C ₁₁ H ₁₃ NO ₆ Co	313.9	19
	C ₁₈ H ₁₈ N ₂ O ₇ Co	432.9	15
	C ₁₉ H ₁₈ N ₃ O ₇ Co	458.9	22
	C ₂₅ H ₂₂ N ₃ O ₇ Co	534.9	24
	C ₂₆ H ₂₂ N ₄ O ₇ Co	560.9	26
	C ₃₃ H ₂₇ N ₅ O ₈ Co	679.9	23
	C ₃₇ H ₃₃ N ₅ O ₁₂ Co ₂	856.8	21
	C ₄₄ H ₃₈ N ₆ O ₁₃ Co ₂	975.8	19
(7)	C ₆ H ₉ O ₃	129	18
	C ₇ H ₉ NO ₃	146	15
	C ₇ H ₉ NO ₃ Cl ₂ Co	284.9	13
	C ₁₄ H ₁₄ N ₂ O ₄ Cl ₂ Co	403.9	14
	C ₁₅ H ₁₄ N ₃ O ₄ Cl ₂ Co	429.9	21
	C ₂₁ H ₁₈ N ₃ O ₄ Cl ₂ Co	505.9	20
	C ₂₂ H ₁₈ N ₄ O ₄ Cl ₂ Co	531.9	22
	C ₂₉ H ₂₃ N ₅ O ₅ Cl ₂ Co	650.9	24
	C ₂₉ H ₂₃ N ₅ O ₅ Cl ₄ Co ₂	780.9	26
	C ₃₆ H ₂₈ N ₆ O ₆ Cl ₄ Co ₂	899.8	24

Table 3. Infrared spectral bands (cm⁻¹) of H₄L ligand and its metal complexes.

No.	$\nu(\text{OH})$	$\nu(\text{C-H})$	$\nu(\text{C=N})$	$\delta(\text{O-H})$ $\gamma(\text{O-H})$	$\nu(\text{C-O})$	$\nu(\text{Ar})_{\text{ring}}$	$\nu(\text{OAc})$	$\nu(\text{M-O})$	$\nu(\text{M-N})$	$\nu(\text{M-Cl})$
(1)	3425	3040-2840	1620, 1570	1385 976	1323	1605, 755	-	-	-	-
(2)	3429	3070 - 2850	1608, 1529	-	1320	1590, 750	-	580	427	-
(3)	3399	3090 - 2865	1617, 1565	1382 972	1321	1570, 745	-	560	480	420
(4)	3430	3085 - 2870	1615, 1567	1383 972	1320	1560, 764	1550, 1349	519	455	-
(5)	3427	3095 - 2795	1617, 1567	1382 971	1319	1573, 753	-	555	468	418
(6)	3424	3055 - 2810	1616, 1567	1383 970	1320	1573, 760	1562, 1415	545	458	-
(7)	3429	3110 - 2825	1613, 1534	1379 965	1301	1565, 770	-	550	450	415

NMR spectra

The ^1H NMR and ^{13}C NMR spectra for compound (**1**) were measured in DMSO-*d*₆. The ^1H NMR spectrum of (**1**) (Figure 3) shows that all the peaks are duplicated due to tautomerization. Peaks at 5.0 ppm belong to the OH protons. The aromatic protons can be observed as multiplet at 8.20–6.80 ppm for 20 hydrogen atoms present at aromatic protons. The ^{13}C NMR spectrum of (**1**) showed peaks appeared at 163.0 ppm refers to hydrazide imine carbon (C=N) as duplicated peak due to tautomerization. While the aromatic carbons CH peaks were at 147.2 and 116.9 ppm.

Mass spectra

The mass spectrum of ligand (**1**) (Table 2) supports the proposed structure with the molecular ion peak at m/z 609. Furthermore, four fragments can be seen. That at m/z 540 belongs to loss of four OH groups from the ligand; the second peak at m/z 391 corresponds to the loss of two phenyl groups; the peak at m/z 225 is expected to be for the loss of other two phenyl groups and the base peak was phenyl group at m/z 77.

Infrared studies

The IR spectral results of [**H₄L**] ligand (**1**), its metal complexes and their assignments are collected in Table (2). The investigation of [**H₄L**] ligand spectrum reveals several fundamental weak-broad bands at 3425; (3040); (2915, 2840) assigned to the O–H stretching mode corresponding to the phenolic hydroxyl group overlapped with adsorbed water molecules; aromatic and aliphatic (C–H), respectively. Also, the spectrum shows a bands at 1620, 1570 and 1323 cm^{-1} assignable to stretching vibration of (C=N) group, $\nu(\text{C}=\text{C})$ and $\nu(\text{C}-\text{O})$ [26 - 28]. The additional bands located at 1385 and 976 cm^{-1} are restricted to $\delta(\text{OH})$ and $\gamma(\text{OH})$.

The Schiff base ligand [**H₄L**] has two ONNO donor sites; therefore, it could react with all metal ions in the molar ratio (2:1) (M:L); M = Cu(II), Ni(II) and Co(II). The ligand coordinates through two azomethine N atoms and two phenolic O atoms with each metal ion in the binuclear complex acts as a neutral ligand except complex (**2**) where the ligand undergo deprotonation before complexation with Cu ion. This is supported through characterization of the metal complexes and suggested by DFT studies. The IR spectra of all metal complexes show a shift in $\nu(\text{C}=\text{N})$ (azomethine) stretching to a lower value by 3–12 cm^{-1} indicating coordination through the azomethine N atoms. The $\nu(\text{OH})$ bands in the complexes remain at the same position as that of the ligand due to overlapping with water of crystallization. However, $\delta(\text{OH})$ and $\gamma(\text{OH})$ bands of the ligand (1383; 976 cm^{-1}) undergo change in their shape and position, 3–7; 3–11 cm^{-1} , respectively, indicating the involvement of phenolic (OH) in coordination in all complexes except complex (**2**). The disappearance of peak at $\delta(\text{OH})$ and $\gamma(\text{OH})$ in complex (**2**) may be attributed to the deprotonation of the ligand before complexation with Cu ion. In addition, the coordination of the phenolic groups with the metal ions can be examined by the $\nu(\text{C}-\text{O})$ stretching mode, which is shifted to lower frequencies in all metal complexes. The coordination of phenolic/enolic O and azomethine N atoms is further supported by the appearance of new nonligand bands between 519–580 and 427–480 cm^{-1} due to the $\nu(\text{M}-\text{O})$ and $\nu(\text{M}-\text{N})$ vibrations in all complexes. The appearance of new nonligand bands between 415–420 cm^{-1} due to the $\nu(\text{M}-\text{Cl})$ [26-28].

UV-Visible spectra and magnetic moment measurements

The UV-Visible spectral data for the ligand and its complexes are listed in (Table 4), which showed three bands in the UV region at 275, 305–335 and 375 nm. The first one is ascribed to intraligand transition in the hydrazide moiety which is nearly at the same position after complexation. The next two bands are ascribed to the $\{n \rightarrow \pi^*\}$ transition of the azomethine and nitro groups. These peaks changed to lower energy on complexation, which indicates the

coordination of these groups with the metal ions. Additionally, the spectra of the complexes revealed new bands in the range 346–418 nm, which can be ascribed to the ligand-to-metal charge transfer (LMCT) transitions [26, 27].

Table 4. The electronic absorption spectral bands (nm) and magnetic moment (BM) for the ligand [H₄L] and its complexes.

No.	λ_{\max} (nm)	μ_{eff} in BM
(1)	275, 335, 375	-
(2)	255, 321, 389, 503, 563, 662	1.72
(3)	283, 304, 380, 455, 532, 645	1.73
(4)	286, 310, 485, 630, 738, 910	2.25
(5)	283, 306, 386, 493, 617, 720	2.37
(6)	287, 295, 390, 535, 635	3.99
(7)	280, 290, 395, 532, 630	3.85

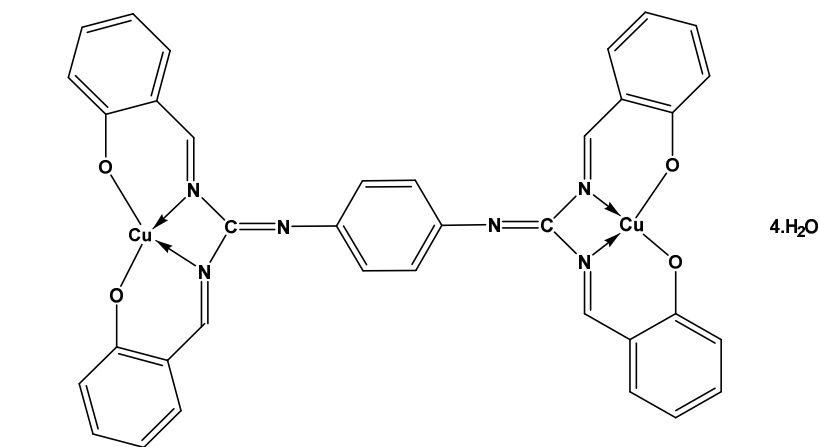
For the Cu²⁺ complex (2) 255, 321 and 389 nm, these bands are within the ligand and bands at 503, 563 and 662 nm are corresponding to ²B_{1g}→²B_{2g}, ²B_{1g}→²E_g and ²B_{1g}→²A_{1g}, respectively, suggesting a square planar geometry [13, 29]. Complex (3) in elongated tetragonally distorted octahedral or square planar geometries of D_{4h} symmetry, three spin-allowed transitions are expected, ²A_{1g}←²B_{1g}, ²B_{2g}←²B_{1g}, ²E_g←²B_{1g}, which appear in the ranges (455, 532, 645) nm, respectively [31]. The transitions indicating that they have a tetragonally distorted octahedral geometry (Figure 1). Sometimes these theoretical explanations are difficult to see in practice due to overlapping and become hard to resolve into separate peaks owing to the slight difference in energy between the d levels. Complexes (2, 3) exhibit magnetic moment values in the 1.72 and 1.73 BM related to spin-only value which confirmed the structure of the complexes. The octahedral geometry of Ni(II) complexes (4, 5) is characterized by spectral bands at 517, (630, 738, 910) and (493, 617, 720)nm attributed to ³A_{2g}(F) → ³T_{1g}(P)v₃, ³A_{2g}(F) → ³T_{1g}(F)v₂ and ³A_{2g}(F) → ³T_{2g}(F)v₁, respectively [29, 31]. Electronic transitions, compatible with an octahedral geometry for the Ni²⁺ ion. This geometry is confirmed by the magnetic nature of these complexes [31, 32]. The Co(II) complexes (6, 7) shows d–d transitions at 506, 534 and 622 nm corresponding to ⁴T_{1g}(F) → ⁴T_{1g}(P), ⁴T_{1g}(F) → ⁴A_{2g}(F) and ⁴T_{1g}(F) → ⁴T_{2g}(F), indicating high-spin octahedral geometry for Co(II) ion [30, 33].

At room temperature magnetic moments of the complexes (2)–(7) are shown in Table (4). Copper(II) complexes (2) and (3) show values 1.72 and 1.73 B.M., corresponding to one unpaired electron in an octahedral geometry however, Nickel(II) complexes (4) and (5) give paramagnetic properties that confirmed t_{2g}⁶ e_g⁴ electronic configuration with no unpaired electrons in an octahedral Ni(II) complexes. Cobalt(II) complexes (6) and (7) give values 3.99 and 3.85 B.M. that confirmed t_{2g}⁶ e_g² electronic configuration with two unpaired electrons in an octahedral Co(II) complexes. Based on elemental analyses and spectral methods, the suggested chemical structures for the synthesized metal complexes are represented in Figure 1.

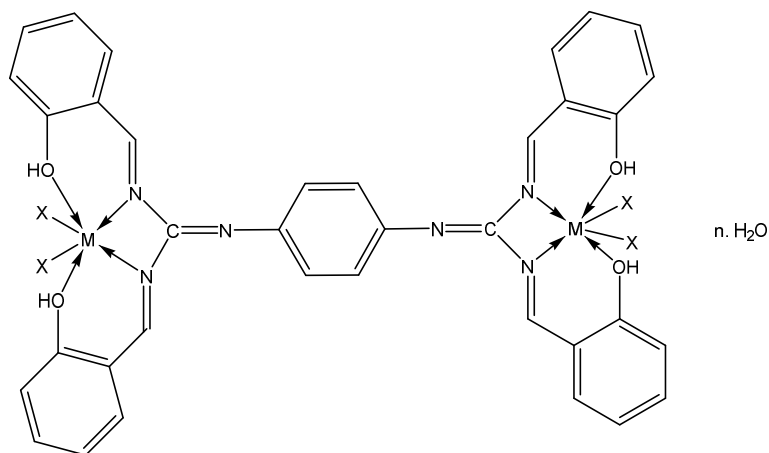
Electron spin resonance (ESR)

The ESR spectral data for complexes (2) and (6) are presented in Table 5. The spectra of copper(II) complex (2) are characteristic of species, d⁹ configuration and having axial type of a d_(x²-y²) ground state which is the most common for copper(II) complexes [34, 35]. The complexes show g_{||} > g_⊥ > 2.0023, indicating octahedral geometry around copper(II) ion [36, 37]. The g- values are related by the expression [36, 38]. G = (g_{||}-2)/(g_⊥-2), if G > 4.0, then, local tetragonal axes are aligned parallel or only slightly misaligned, if G < 4.0, the significant exchange coupling is present. Complex (2) shows values indicating spin – exchange interactions take place between copper(II)

ions. This phenomenon is further confirmed by magnetic moments values. Also, the $g_{\parallel}/A_{\parallel}$ values considered as a diagnostic of stereochemistry [39], in the range reported for tetragonal distorted octahedral complexes 150 to 250 cm^{-1} . The calculated orbital publications for the cobalt(II) complexes (**6**) indicates a $d_{(x^2-y^2)}$ ground state [40] which shows isotropic spectra with values 2.15 confirmed octahedral structure [35, 40].



Complex (2)



No.	M	X	N
3	Cu(II)	Cl	2
4	Ni(II)	OAc	1
5	Ni(II)	Cl	3
6	Co(II)	OAc	1
7	Co(II)	Cl	2

Figure 1. Structure of complexes (2-7).

Table 5. ESR data for the metal (II) complexes.

No.	$g_{ }$	g_{\perp}	g_{iso}^a	$A_{ }$ (G)	A_{\perp} (G)	A_{iso}^b (G)	G^c	ΔE_{xy}	ΔE_{xz}	K_{\perp}^2	$K_{ }^2$	K	$g_{ }/A_{ }$	α^2	β^2	β_1^2	-2β	a_d^2 (%)
(2)	2.18	2.03	2.07	125	25	63	3.6	16220	20615	0.46	0.57	0.72	173.8	0.58	1.23	1.01	-275	82.3
(6)	-	-	2.15	-	-	-	-	-	-	-	-	-	-	-	-	-	--	-

a) $g_{iso} = (2g_{\perp} + g_{||})/3$, b) $A_{iso} = (2A_{\perp} + A_{||})/3$, c) $G = (g_{||} - 2)/(g_{\perp} - 2)$.

Table 6. Thermal data for some of metal complexes.

Complex No.	Temp. (°C)	DTA (peak)		TGA (wt. loss)		Assignments
		Endo	Exo	Calc.	Found	
Complex (2)	45	Endo	-	-	-	Broken of H-bondings
	70	Endo	-	1.83	1.46	Loss of (H ₂ O) hydrated water molecule
	160	Endo	-	24.51	24.29	Loss of coordinated four (OAc) groups
	350	-	Exo	-	-	Melting point
	460 - 650	-	Exo	21.87	21.33	Decomposition process with formation of two CuO
Complex (3)	45	Endo	-	-	-	Broken of H-bondings
	80	Endo	-	3.96	3.65	Loss of (2H ₂ O) hydrated water molecules
	210	Endo	-	16.27	16.08	Loss of coordinated four (Cl) molecules
	325	Exo	-	-	-	Melting point
	435 - 660	-	Exo	21.75	21.12	Decomposition process with the formation of two CuO
Complex (4)	40	Endo	-	-	-	Broken of H-bondings
	75	Endo	-	1.85	1.58	Loss of (H ₂ O) hydrated water molecule
	170	Endo	-	24.66	24.57	Loss of coordinated four (OAc) groups
	335	Endo	-	-	-	Melting point
	455 - 675	-	Exo	20.69	20.72	Decomposition process with the formation of two NiO
Complex (5)	44	Endo	-	-	-	Broken of H-bondings
	80	Endo	-	5.89	5.75	Loss of (3H ₂ O) hydrated water molecules
	165	Endo	-	16.45	16.18	Loss of four (Cl) molecules
	315	Exo	-	-	-	Melting Point
	430 - 680	-	Exo	20.69	20.81	Decomposition process with the formation of two NiO
Complex (6)	46	Endo	-	-	-	Broken of H-bondings
	80	Endo	-	1.84	1.17	Loss of (H ₂ O) hydrated water molecule
	175	Endo	-	24.64	24.52	Loss of four (OAc) acetate groups
	320	Exo	-	-	-	Melting Point
	430 - 685	-	Exo	20.75	20.68	Decomposition process with the formation of two CoO
Complex (7)	48	Endo	-	-	-	Broken of H-bondings
	70	Endo	-	4.0	4.17	Loss of two (H ₂ O) hydrated water molecules
	185	Endo	-	16.44	16.52	Loss of four (Cl) molecules
	360	Exo	-	-	-	Melting Point
	430 - 680	-	Exo	20.75	20.78	Decomposition process with the formation of two CoO

Thermal analyses

In order to obtain further information about the thermal stability as well as the nature of water molecules associated with the complex structures, DTA and TGA techniques were applied on complexes (2-7) in the temperature range 25–800 °C. The results of the thermal analyses are presented in Table 6. The thermal data revealed that the calculated weight loss and proposed formula are in agreement and indicated that the complexes are mostly decomposed in two, three or four stages that can be interpreted as following: (i) Dehydration of all complexes takes place in the range 40–80 °C with weight loss ranging from 1.83 (1.46) to 5.59 (5.75) % corresponding to removal of hydrated water molecules according to the complex structures (Table 6). (ii) The second step is related to the removal of acetate, or chloride anions from complexes (2-7) takes place at 160–185 °C which can be confirmed from the percentage of weight loss (Table 6). (iii) The last step is the complete degradation of complexes (2-7) through loss of the organic part at 430–680 °C leaving the metal oxide which can be confirmed from the percentage weight loss (Table 6). All complexes passing the melting point which pointed in (Table 6) without any weight loss.

Table 7. Antimicrobial activities of ligand and its complexes against *A. niger* and *E. coli*.

Compound	<i>A. niger</i> Inhibition zone (mm)	Activity index (%)	<i>E. coli</i> Inhibition zone (mm)	Activity index (%)
DMSO	0	0	0	0
Amphotericin B	17	100	0	0
Tetracycline	0	0	37	100
1	15	88.2	10	27
2	15	88.2	15	40.5
3	23	138.2	20	54.1
4	13	67.5	20	54.1
5	20	117.5	22	59.5
6	12	32.4	18	48.6
7	18	105.9	23	62.2

Biological activity

The well diffusion method at 10 mg mL⁻¹ concentration in DMSO was used to measure the antimicrobial activity against *A. niger* and *E. coli*. The results (Table 7) showed that ligand (1) has activity similar to that of the antifungal drug amphotericin B with a 17 mm inhibition zone, while some of the synthesized complexes (2–7) were more active than amphotericin B. The most active complex was the copper chloride one (3) with a 23 mm inhibition zone (activity index (AI) = 138.2%), and the second most active was nickel(II) complex (5) with a 20 mm inhibition zone (AI = 122.3%). The rest of the complexes showed activity in the range 13–18 mm. The order of antifungal activity is shown in Figure 2. In the case of antibacterial activity against *E. coli*, ligand (1) does not show any activity in comparison with tetracycline as an antibacterial with a 37 mm inhibition zone. The prepared complexes showed good to moderate activity. The reason for this order is strongly related to the lipophilicity of the central metal ion obtained based on Overton's and Tweedy's chelation connotation and theory. In conformity with Overton's concept of cell permeability, the lipophilic soluble complexes are allowed to pass through the cell membrane since the liposolubility is a key factor which affects antimicrobial activity. On coordination, the metal ion polarity becomes restrained to a great extent due to interference of the ligand orbital and partial sharing of the positive charge of the metal ion with donor groups. Moreover, it promotes the distribution of π -electrons through the chelating ring and enhances the complex

lipophilicity, as a result increasing the penetrating ability of the complexes through the lipid membranes and blocking the metal binding sites of cell enzymes. The synthesized complexes also have an effect on the respiration process of the cell which leads to a blocking of the generation of proteins, which affects the growth of microbe cells [46-51].

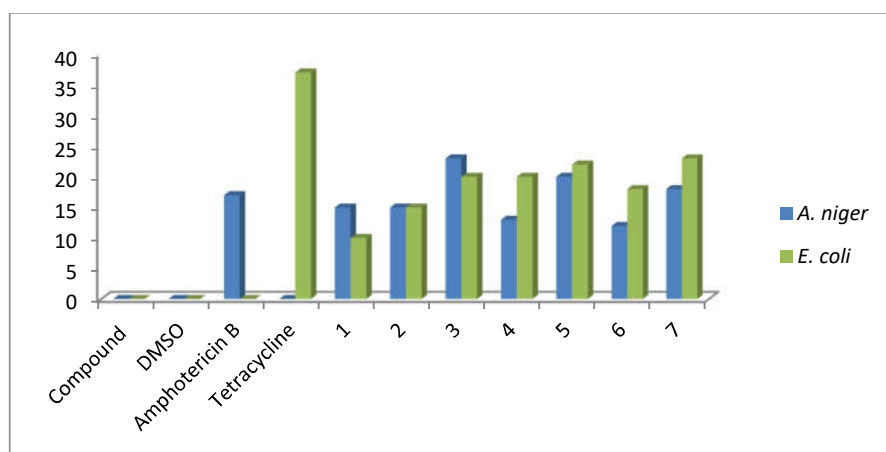


Figure 2. Order of antifungal and antibacterial activities of ligand and its complexes against *A. niger* and *E. coli*.

CONCLUSION

Novel Cu(II), Ni(II) and Co(II) complexes of multidentate Schiff base ligand were prepared. These complexes have been characterized by ^1H NMR, mass spectra, IR, UV-Vis, ESR spectra, magnetic moments, and conductance measurements, as well as, elemental and thermal analyses (DTA and TGA). The new complexes were non-electrolytes, non-hygroscopic and were dissolvable in DMSO but insoluble in common natural solvents. Out of the 6 complexes, Cu(II), Ni(II) and Co(II) complexes enhanced biological activities against G+ve and G-ve bacteria and against fungi with very rare cytotoxic effects on normal cells in comparison to the parent ligand and to the standard drug indicating their promising antimicrobial agents.

REFERENCES

1. Renfrew, A.K. Transition metal complexes with bioactive ligands: Mechanisms for selective ligand release and applications for drug delivery. *Metallomics* **2014**, 6, 1324-1335.
2. Baron, R.; Binder, A.; Wasner, G. Neuropathic pain: Diagnosis, pathophysiological mechanisms, and treatment. *Lancet Neurol.* **2010**, 9, 807-819.
3. Selvaganapathy, M.; Raman, N. Pharmacological activity of a few transition metal complexes: A short review. *J. Chem. Biol. Ther.* **2016**, 2, 108.
4. Mohamed, G.G.; Omar, M.; Hindy, A.M. Synthesis, characterization and biological activity of some transition metals with Schiff base derived from 2-thiophene carboxaldehyde and aminobenzoic acid. *Spectrochim. Acta Part A Mol. Biomol. Spectrosc.* **2005**, 62, 1140-1150.
5. Reddy, A.K.; Kathale, N.E. Synthesis and anti-inflammatory activity of hydrazones bearing biphenyl moiety and vanillin based hybrids. *Orient. J. Chem.* **2017**, 33, 971-978.
6. El-Tabl, A.S.; Mohamed Abd El-Waheed, M.; Wahba, M.A.; El-Fadl, A.E.-H.A. Synthesis, characterization, and anticancer activity of new metal complexes derived from 2-hydroxy-3-

- (hydroxyimino)-4-oxopentan-2-ylidene) benzohydrazide. *Bioinorg. Chem. Appl.* **2015**, 201, 126023.
7. Wen, A.M.; Steinmetz, N.F. Design of virus-based nanomaterials for medicine, biotechnology, and energy. *Chem. Soc. Rev.* **2016**, 45, 4074-4126.
 8. Ahmad, F.; Taj, M.; Tirmizi, S.; Alelwani, W.; Hajjar, D.; Makki, A.; Shah, S.; Ali, U.; Hassan, U.; Tahir, M. Selective complexation of hydrazone based ketimine with 3d, 4d, and 5d metals: Synthesis, characterization, and biological activity. *Russ. J. Gen. Chem.* **2019**, 89, 142-147.
 9. Juje, F.A.; Jayaprakash, H. Synthesis, characterization and biological importance of acid hydrazone complexes. *Int. J. Adv. Res. Dev.* **2017**, 2, 61-65.
 10. Kendur, U.; Chimmalagi, G.H.; Patil, S.M.; Gudasi, K.B.; Frampton, C.S. Synthesis, structural characterization and biological evaluation of mononuclear transition metal complexes of zwitterionic dehydroacetic acid N-arylohydrazone ligand. *Appl. Organomet. Chem.* **2018**, 32, e4278.
 11. Noor, S.; Rashid, M.A. Solubilization and thermodynamic attributes of nickel phenanthroline complex in micellar media of sodium 2-ethyl hexyl sulfate and sodium bis (2-ethyl hexyl) sulfosuccinate. *Tenside Surfactants Deterg.* **2019**, 56, 490-498.
 12. Noor, S.; Younas, N.; Rashid, M.A.; Nazir, S.; Usman, M.; Naz, T. Spectroscopic, conductometric and biological investigation of [Ni(phen)₃]F₂.EtOH.MeOH.8H₂O complex in anionic micellar media. *Colloid Interface Sci. Commun.* **2018**, 27, 26-34.
 13. Taj, M.B.; Alkahtani, M.D.; Ali, U.; Raheel, A.; Alelwani, W.; Alnajeebi, A.M.; Babteen, N.A.; Noor, S.; Alshater, H. New heteroleptic 3d metal complexes: Synthesis, antimicrobial and solubilization parameters. *Molecules* **2020**, 25, 4252.
 14. Taj, M.; Raheel, A.; Alelwani, W.; Hajjar, D.; Makki, A.; Alnajeebi, A.; Babteen, N.; Tirmizi, S.; Noor, S. A swift one-pot solventfree synthesis of benzimidazole derivatives and their metal complexes: Hydrothermal treatment, enzymatic inhibition, and solubilization studies. *Russ. J. Gen. Chem.*, **2020**, 90, 1533-1543.
 15. Younas, N.; Rashid, M.A.; Usman, M.; Nazir, S.; Noor, S.; Basit, A.; Jamil, M. Solubilization of Ni imidazole complex in micellar media of anionic surfactants, sodium dodecyl sulfate and sodium stearate. *J. Surfactants Deterg.* **2017**, 20, 1311-1320.
 16. Hanif, S.; Usman, M.; Hussain, A.; Rasool, N.; Zubair, M.; Rana, U.A. Solubilization of benzothiazole (BNZ) by micellar media of sodium dodecyl sulfate and cetyl trimethylammonium bromide. *J. Mol. Liq.* **2015**, 211, 7-14.
 17. Masoud, M.S.; El-Marghany, A.; Orabi, A.; Ali, A.E.; Sayed, R. Spectral, coordination and thermal properties of 5-arylidene thiobarbituric acids. *Spectrochim. Acta A* **2013**, 107, 179-187.
 18. Al-Jibouri, M.N. Synthesis and characterization of transition metal complexes with azo ligand derived from 4-hydroxyl-6-methyl-2-pyranone. *Eur. Chem. Bull.* **2014**, 3, 447-451.
 19. Emam, S.M.; Abouel-Enein, S.A.; Abouzayed, F.I. Synthesis, spectral characterization, thermal studies and biological activity of (Z)-5-((1,5-dimethyl-3-oxo-2-phenyl-2,3-dihydro-1H-pyrazol-4-yl)diazanyl)-6-hydroxy-2-mercaptopyrimidin-4(3H)-one and its metal complexes. *Appl. Organometal. Chem.* **2017**, e4073
 20. Youssef, N.S.; Hegab, K.H. Factors affecting the Islamic purchasing behavior – a qualitative study. *J. Mater. Sci. Technol.* **1999**, 5, 263.
 21. Abdel-Monem, Y.K.; Emam, S.M.; Okda, H.M.Y. Solid state thermal decomposition synthesis of CuO nanoparticles from coordinated pyrazolopyridine as novel precursors. *J. Mater. Sci. Mater. Electron.* **2017**, 28, 2923-2934.
 22. Ibrahim, A.R. Preparation and characterization of some transition metal complexes of bis Schiff base ligand. *Int. J. Adv. Res.* **2015**, 3, 315-324.

23. Ali, A.A.; Fahad, T.A.; Abdullah, W.A. Synthesis and spectral characterization of some transition metal complexes of azo-Schiff base derivative of metoclopramide. *J. Adv. Chem.* **2014**, *11*, 3382-3393.
24. Buldurun, K.; Gündüz, B.; Turan, N.; Çolak, N. Synthesis, characterization, optical transition and dielectric properties of the Schiff base ligand and its cobalt(II) and palladium(II) complexes. *J. Electron. Mater.* **2019**, *48*, 7131-7138.
25. Akbari, A.; Hosseini-Nia, A. Biological evaluation and simple method for the synthesis of tetrahydrobenzo[a]xanthenes-11-one derivatives. *J. Saudi Chem. Soc.* **2017**, *21*, S7-S11.
26. Chauhan, H.P.S.; Bakshi, A. Synthetic, spectroscopic, thermal, and structural studies of antimony(III) bis(pyrrolidinedithiocarbamate)alkylidithiocarbonates. *J. Therm. Anal. Calorim.* **2010**, *105*, 937-946.
27. Al Zoubi, W.; Al-Hamdani, A.; Ahmed, S.D.; Gun Ko, Y. Synthesis, characterization and biological activity of Schiff bases metal complexes. *J. Phys. Org. Chem.* **2017**, *31*, e3752.
28. Al-Saif, F.A. Spectroscopic, molar conductance and biocidal studies of Pt(IV), Au(III) and Pd(II) chelates of nitrogen and oxygen containing Schiff base derived from 4-amino antipyrine and 2-furaldehyde. *Int. J. Electrochem. Sci.* **2013**, *8*, 10424-10445.
29. Chandra, S.; Jain, D.; Sharma, A.K.; Sharma, P. Coordination modes of a Schiff base pentadentate derivative of 4-aminoantipyrine with cobalt(II), nickel(II) and copper(II) metal ions: Synthesis, spectroscopic and antimicrobial studies. *Molecules* **2009**, *14*, 174-190.
30. Abd-ElRazek, S.E.; El-Gamasy, S.M. New benzoyl acetohydrazone based metal complexes with viral DNA binding and cleavage and antimicrobial treatments: Synthesis and biological activities. *J. Mol. Struct.* **2023**, *1274*, 134457.
31. Atkin, R.; Brewer, G.; Kokot, E.; Mochier, G.M.; Sinn, E. The synthesis and characterization of nucleotide complexes involving an asymmetric metal. *Inorg. Chim. Acta Bioinorg. Chem.* **1985**, *106*, 37-41.
32. El-Boraey, H.A.; Mansour, A.I. Synthesis, characterization and spectral studies on some new N,N'-pyridine-2,6-diylbis(2-aminobenzamide) metal complexes. *J. Chem. Sci.* **2017**, *7*, 381-390.
33. El-Boraey, H.A.; Emam, S.M.; Tolan, D.A.; El-Nahas, A.M. Structural studies and anticancer activity of a novel (N6O4) macrocyclic ligand and its Cu(II) complexes. *Spectrochim. Acta A* **2011**, *78*, 360-370.
34. El-Gamasy, S.M.; Abd-El Razek, S.E. 4N donor atoms moiety of transition metal complexes of a Schiff base ligand: Synthesis, characterization and biological activities study. *Egypt. J. Chem.* **2021**, *64*, 5975-5987.
35. Mohamed, G.G.; Omar, M.M.; Ibrahim, A.A. Biological activity studies on metal complexes of novel tridentate Schiff base ligand. Spectroscopic and thermal characterization. *Eur. J. Med. Chem.* **2009**, *44*, 4801-4812.
36. Mavrova, A.T.; Wesselinova, D.; Tsenov, Y.A.; Denkova, P. Synthesis, cytotoxicity and effects of some 1,2,4-triazole and 1,3,4-thiadiazole derivatives on immunocompetent cells. *Eur. J. Med. Chem.*, **2009**, *44*, 63-69.
37. Abd El-Razek, S.E.; El-Gamasy, S.M.; Hassan, M.; Abdel-Aziz, M.S.; Nasr, S.M. Transition metal complexes of a multidentate Schiff base ligand containing guanidine moiety: Synthesis, characterization, anti-cancer effect, and anti-microbial activity. *J. Mol. Struct.* **2019**, *1203*, 127381.
38. Mahmoud, W.H.; Mohamed, G.G.; El-Dessouky, M.M.I. Synthesis, characterization and in vitro biological activity of mixed transition metal complexes of lornoxicam with 1,10-phenanthroline. *Int. J. Electrochem. Sci.* **2014**, *9*, 1415-1438.
39. Vojinović-Ješić, L. S., Rodić, M., Hollo, B. B., Synthesis, characterization and thermal behavior of copper(II) complexes with pyridoxal thiosemi (PLTSC)- and S-methylisothiosemicarbazone (PLITSC). *J. Therm. Anal. Calorim.* **2015**, *123*(3). DOI 10.1007/s10973-015-4891-7.

40. Abdel-Rahman, L.H.; Ismail, N.M.; Ismail, M.; Abu-Dief, A.M.; Ahmed, E.A.H. Synthesis, characterization, DFT calculations and biological studies of Mn(II), Fe(II), Co(II) and Cd(II) complexes based on a tetradentate ONNO donor Schiff base ligand. *J. Mol. Struct.* **2017**, 1134, 851-862.
41. Bertrand, J.A.; Black, T.D.; Eller, P.G.; Helm, F.T.; Mahmood, R. Polynuclear complexes with hydrogen-bonded bridges. Dinuclear complex of N,N'-bis(2-hydroxyethyl)-2,4-pentanediamine with copper(II). *Inorg. Chem.* **1976**, 15, 2965-2970.
42. Geary, W.J. The use of conductivity measurements in organic solvents for the characterisation of coordination compounds. *Coord. Chem. Rev.* **1971**, 7, 81-122.
43. Karlin, K.D.; Hayes, J.C.; Hutchinson, J.P.; Zubieta, J. Model complexes for ligand probes of Met-hemocyanin and Met-tyrosinase derivatives. Structure of a novel 1,1-azido bridged binuclear copper(II) complex. *J. Chem. Soc. Commun.* **1983**, 376-378.
44. Hathaway, B.; Billing, D. The electronic properties and stereochemistry of mono-nuclear complexes of the copper(II) ion. *Coord. Chem. Rev.* **1970**, 5, 143-207.
45. Al-Hakimi, A.N.; A.S. El-Tabl; Shakhdofo, M.M. Coordination and biological behaviour of 2-(*p*-toluidino)-N'-(3-oxo-1,3-diphenylpropylidene) acetohydrazide and its metal complexes. *J. Chem. Res.* **2009**, 12, 770-774.
46. Hathaway, B. The electronic properties and stereochemistry of the copper(II) ion. Part VI. Bis(bipyridyl)copper(II) complexes. *J. Chem. Soc. A: Inorg. Phys. Theor.* **1969**, 2219-2224.
47. Smith, D. Chlorocuprates(II). *Coord. Chem. Rev.* **1976**, 21, 93-158.
48. Kivelson, D.; Neiman, R. ESR studies on the bonding in copper complexes. *J. Chem. Phys.* **1961**, 35, 149-155.
49. Xiong, Y.; He, X.; Zou, X.; Wu, J.; Chen, X.; Ji, L.; Li, R.; Zhoub, J.; Yuc, K. Interaction of polypyridyl ruthenium(II) complexes containing non-planar ligands with DNA. *J. Chem. Soc., Dalton Trans.* **1999**, 19-24.
50. Andrews, R.K.; Blakeley, R.L.; Zerner, B. *Transition-Metal Storage, Transport, and Biomineralization, The Bioinorganic Chemistry of Nickel*, Vol. 141, Lancaster, J.R. (Ed), VCH Publishers: New York; **1988**.